Soft Matter

PAPER

View Article Online
View Journal | View Issue

Cite this: *Soft Matter*, 2014, **10**, 3134

Collapse from the top: brushes of poly-(*N*-isopropylacrylamide) in co-nonsolvent mixtures†

Qi Chen,[a] E. Stefan Kooij,[b] Xiaofeng Sui,[a] Clemens J. Padberg,[a] Mark A. Hempenius,[a] Peter M. Schön[a] and G. Julius Vancso*[a]

Using a combination of ellipsometry and friction force microscopy, we study the reversible swelling, collapse and variation in friction properties of covalently bound poly(*N*-isopropylacrylamide) (PNIPAM) layers on silicon with different grafting densities in response to exposure to good solvents and co-nonsolvent mixtures. Changes in the thickness and segment density distribution of grafted films are investigated by *in situ* ellipsometry. Based on quantitative modelling of the ellipsometry spectra, we postulate a structural model, which assumes that collapse takes place in the contacting layer between the brush and the co-nonsolvent and the top-collapsed brushes remain hydrated in the film interior. Using the structural model derived from ellipsometry spectra, we analyse the AFM based friction force microscopy data, which were obtained by silica colloidal probes. Results show a large increase of the friction coefficient of PNIPAM grafts when the grafts swollen by water are brought in contact with co-nonsolvents. For instance, the value of the friction coefficient for a medium density brush in water is four times lower than the value observed in a water–methanol (50% v/v) mixture. This increase of friction is accompanied by an increase in adherence between the PNIPAM chains and the silica colloidal probes, and is a result of chain collapse in the graft when contacted by a co-nonsolvent mixture in agreement with the model postulated on the basis of ellipsometric characterisation. The kinetic behaviour of the collapse is assessed by measuring the temporal variation of friction *in situ* as a function of elapsed time following contact with the co-nonsolvent as a function of graft density. In conclusion, the effect of co-nonsolvency influenced both the thickness of the PNIPAM brushes and the tribological behavior of the brush surfaces.

Received 24th January 2014
Accepted 28th January 2014

DOI: 10.1039/c4sm00195h

www.rsc.org/softmatter

Introduction

Stimuli responsive polymer grafts can be used for a wide variety of applications in the areas of actuation, sensing, cell culture regulation, controlled drug delivery, micro- and nanofluidics, and in many other fields.[1–8] Poly(*N*-isopropylacrylamide) (PNIPAM) grafts have been widely studied due to the reversible phase transition they exhibit in aqueous solutions at the lower critical solution temperature (LCST) of 32 °C. PNIPAM chains show strong hydration behaviour below the LCST, while above the LCST, they adopt a collapsed conformation (coil-to-globule transition).[9,10] Changes in the external environment (*e.g.* temperature, solvent composition) can trigger a sharp and large response in the structure and properties of grafted PNIPAM polymer films. For example, it was shown that the value of the LCST depends on the chain length and grafting density.[11] Interestingly, single chain PNIPAM AFM force spectroscopy experiments did not carry a fingerprint of the LCST.[12] PNIPAM grafts are interesting candidates for applications in, *e.g.* permeation-controlled filters, tissue engineering and as actuators and valves in fluidics, among other areas.[13,14] The influence of temperature on the polymer structure and hydration of surface grafted PNIPAM films is well documented in the literature.[11,15–27]

PNIPAM is also known to exhibit co-nonsolvency behavior, *i.e.* solvation responsiveness to the variation in the composition of mixed solvents consisting of water and certain water-miscible organic solvents such as alcohols.[28–37] Napper *et al.* reported coil-to-globule transitions in mixed dispersion media of PNIPAM chains at latex interfaces.[38] The authors noted that upon isothermal addition of lower alcohols to PNIPAM in aqueous systems the chains collapsed and then became swollen again upon further increase of the alcohol concentration. The

[a]*Department of Materials Science and Technology of Polymers, University of Twente, MESA+ Institute for Nanotechnology, P.O. Box 217, 7500 AE Enschede, The Netherland. E-mail: g.j.vancso@utwente.nl; Fax: +31 53 489 3823; Tel: +31-53-4892967*

[b]*Physics of Interfaces and Nanomaterials, MESA+ Institute for Nanotechnology, University of Twente, P.O. Box 217, 7500AE Enschede, The Netherlands*

† Electronic supplementary information (ESI) available: Analysis of ellipsometry spectra and lateral force constant calibration. See DOI: 10.1039/c4sm00195h

reversible collapse and re-swelling has been referred to as re-entry transition. Brushes exhibiting co-nonsolvency behaviour in certain solvent mixtures are highly swollen in either of the pure solvents but collapsed in their mixtures between two specific solvent compositions. As is well known, both pure water and methanol are good solvents for PNIPAM. To understand PNIPAM solubility one must consider the delicate balance in the various contributions to molecular interactions including formation of H-bonds between water or methanol and the amide groups in the polymer, as well as solvent cluster effects. For the occurrence of LCST, hydrophobic effects are also important.[28] For instance, in a water–methanol (50% v/v) PNIPAM ternary system at room temperature, the solvent–solvent interaction due to the formation of water–methanol complexes is stronger than the solvent–polymer interactions, leading to the desolvation of PNIPAM.[33]

In a previous study,[39] we measured adhesion of PNIPAM grafts to an atomic force microscope (AFM) colloidal probe during the collapse of the brush induced by the addition of a co-nonsolvent. Young's moduli values of PNIPAM grafts under different solvent conditions were estimated based on the Hertz model using AFM force–distance curves.

However, detailed studies on swelling, collapse and expected related variations on the friction properties of PNIPAM layers with different grafting densities under varied solvent conditions have not been reported. In view of the applications of PNIPAM as a designer stimulus responsive graft polymer platform in surface engineering, it is of great interest to perform in-depth studies aiming at variations of film morphology, and as a result tribological properties of such layers that accompany the thickness changes when the grafted films are brought into contact with co-nonsolvents.

In this work, the thickness changes due to the swelling and collapse of PNIPAM layers are studied by *in situ* spectroscopic ellipsometry.[40] Subsequently, AFM based lateral force microscopy[41–43] is employed to investigate the friction coefficient in response to changing the solvent environment from a good solvent (water) to a non-solvent (water–methanol) under isothermic (room temperature) conditions. The structural model derived from the ellipsometry measurements provides the basis for the analysis and interpretation of the AFM results.

Ellipsometry comprises a powerful, non-invasive optical probe enabling characterization of bulk materials as well as thin films and provides information on structural and optical properties of surface bound films. As such, it has been widely used for studies of polymer grafts under different solvent conditions.[44–50] As an example, Edmondson *et al.*[44] performed *in situ* spectroscopic ellipsometry measurements to study the co-nonsolvency effect, *i.e.* the collapse in a mixed water–methanol solvent, of high density poly(2-(methacryloyloxy)ethylphosphorylcholine) (PMPC) brushes. Their results show that the judicious selection of the model used to describe the structure of surface bound films is essential for extracting meaningful structural information. These authors found that the best fits to the data were obtained using an exponential decay of polymer density as a function of distance from the substrate surface. Recently, we have described a similar model to account for the temperature-induced conformational changes in 'grafted from' PNIPAM brushes, obtained by surface-initiated polymerization.[50] To adequately account for the optical response at temperatures below and above the LCST, we adopted a two-layer model with a dense layer near the substrate and a more dilute layer on the side of the film exposed to the liquid.

Since the pioneering work of Klein *et al.*, showing that polymer brushes dramatically reduce friction, tribological properties of grafts have attracted tremendous attention.[69] For brush lubrication studies the surface forces apparatus (SFA) has been used with great success. However, measurements by AFM based friction force microscopy (FFM) provide quantitative tribological information concerning polymer graft properties, accompanied by surface morphology imaging.[41–43,51,52] For instance, greatly enhanced lubrication for poly(2-(dimethylamino)ethyl methacrylate) was observed at low pH, which was attributed to the formation of a repulsive, highly charged, hydrated cushion.[53] In a recent study,[54] the frictional properties of high density PMPC brushes under co-nonsolvency conditions were described and substantially increased friction coefficients were observed in ethanol/water (90% v/v) mixtures.

Combination of a detailed characterization of the reversible change of film thickness with the friction force enables a quantitative discussion of the collapse dynamics in relation to the grafting density. Based on the optical response, a model is proposed to explain variations in the brush segment density in the surface-normal directions of the grafts, which agrees well with the observed variation of the friction coefficients when hydrated, swollen brushes are brought in contact with co-nonsolvent mixtures.

Experimental

Materials

PNIPAM grafts with three different grafting densities, termed high, medium and low density (hereafter HD, MD and LD) surfaces, respectively, were synthesized *via* surface-initiated atom transfer radical polymerization (SI-ATRP; see Scheme 1). The preparation of the PNIPAM grafts on silicon was carried out as described in detail in our previous study.[39]

Dry brush thicknesses were 10 nm for LD, 100 nm for MD and 240 nm for HD surfaces as determined from AFM height measurements. The estimated corresponding grafting densities were 0.03 [chains nm^{-2}] for the LD, 0.27 [chains nm^{-2}] for the MD and 0.69 [chains nm^{-2}] for the HD surface, respectively.[39]

Measurements

All experiments were performed at room temperature. The optical characteristics of the brush films were obtained using a Woollam variable angle spectroscopic ellipsometer (VASE) system. Measurements were performed as a function of photon energy in the range of 1.5–4.5 eV with a step size of 0.1 eV; this corresponds to a wavelength range of 275–827 nm. All measurements were performed *in situ* using a custom-built dedicated liquid cell. Optical access to the sample was achieved through two windows at a fixed angle of incidence $\theta = 63°$. A

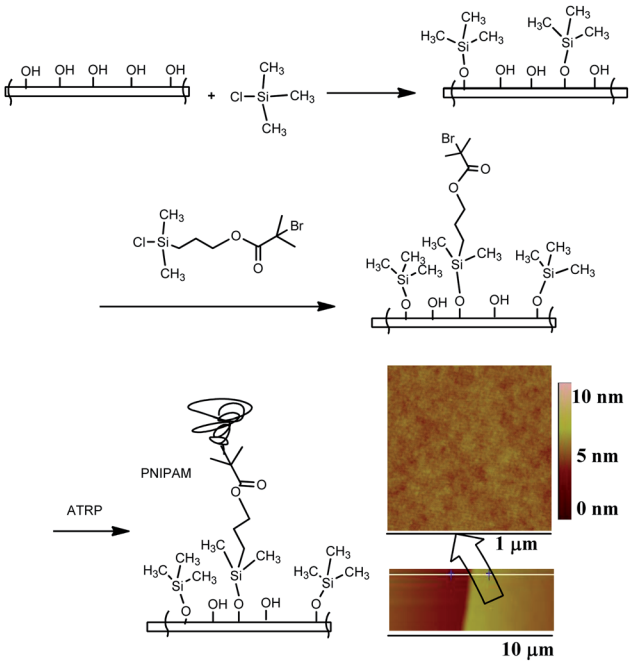

Scheme 1 Schematic representation of grafting PNIPAM films from silicon substrates.

third window enabled alignment of the sample at normal incidence and allowed visual inspection of the sample during *in situ* experiments. The ellipsometry spectra, *i.e.* Ψ and Δ as a function of wavelength, were analysed using CompleteEASE (Woollam), employing tabulated dielectric functions for bulk silicon, silicon dioxide and water.[55] Details pertaining to the data analysis and optical modelling are provided in the ESI.†

A Dimension D3100 AFM (Digital Instruments, Veeco-Bruker, Santa Barbara, CA) was operated in the tapping mode to obtain the thickness and surface morphology of PNIPAM brushes. The PNIPAM grafts were scratched by tweezers and the height differences between the unscratched and the scratched regions were measured to determine the layer thickness.

Force measurements were performed in the liquid environment using a NanoScope IIIa multimode AFM (Digital Instruments, Veeco-Bruker, Santa Barbara, CA) equipped with a standard liquid cell. A silica colloidal probe (Novascan Technologies, Inc. Ames, IA, USA) with a spring constant of 0.050 ± 0.003 N m^{-1} (determined using the thermal tune method)[56] and a diameter of 0.9 μm (as determined by SEM and scanning a tip array[57]) was used in the experiments. Quantitative friction measurements were taken from friction loops acquired by obtaining forward–reverse scan cycles along a single line with the AFM employed in scope mode. The friction signal was obtained by subtracting the mean signals in both directions, giving a resultant force that was twice the frictional force. In each measurement, the vertical signal (deflection setpoint) was first minimized to zero and then increased stepwise up to 10 V. Multiple repeat measurements were made at different locations on the samples to verify that the system was stable and provided reproducible data. The maximum range for the photo-detector is −10 V to +10 V. The maximum force (~80 nN) we recorded in our experiments corresponded to a signal readout of ~600 mV. This is well within the linear range of the detector; we did not observe any non-linearities.

The torsional spring constant ($k_\phi = 5.24 \times 10^{-10}$ Nm rad^{-1}) of the colloidal probe was calculated from the geometry, dimensions and material properties of the V-shaped cantilever and the SiO_2 bead according to the analytical approach of Sader *et al.*[58] This corresponds to a lateral spring constant of k_L = 380 N m^{-1}. Dimensions of the cantilever and the SiO_2 bead were determined from SEM measurements. An elastic modulus of 185 GPa and a Poisson ratio of 0.25 for Si_3N_4 was used for the calculation of the lateral spring constant.[59] The torsional sensitivity (S_ϕ = 0.29 mrad V^{-1}, or its reciprocal value 3.45 × 10^3 V rad^{-1}) was derived from the lateral photodiode sensitivity (0.34 nm V^{-1}), which in turn was determined from the measured vertical photodiode responsivity (73.3 nm V^{-1}) in aqueous buffer and the dimensions of the cantilever. Here the assumption was made that under identical small displacements in normal and lateral directions a linear relationship between the corresponding normal and lateral voltage signals can be approximated.[59] Further details on the torsional sensitivity and spring constant calculation are provided in a separate paragraph in the ESI.†‡

The solvent environment was varied by gently injecting Milli-Q grade water or a water–methanol mixture (50% v/v) into the AFM liquid cell from the outlet within 5 s using a syringe.

Optical characterization by ellipsometry: variation of the brush morphology across the re-entry transition

In order to assess changes in the morphology of the graft layers, we monitored the film thickness variation in different solvents (water and water–methanol, 50% v/v) by *in situ* ellipsometry. In reflection ellipsometry, the change in the polarization state of linearly polarized light is measured upon reflection at an interface. The complex reflection coefficient ρ is defined as:

$$\rho = \frac{r_p}{r_s} = \tan\ \Psi\ \exp(i\Delta)$$

where r_p and r_s are the complex reflection coefficients for the parallel and perpendicular polarizations, respectively. Historically, the quantity ρ is expressed in two angles Ψ and Δ.[60]

Ellipsometry spectra for the PNIPAM layers with different grafting densities are shown in Fig. 1. Spectra are shown for dry samples (squares), samples in contact with a mixture of water–methanol (50% v/v) (circles) and in pure water (triangles). For the LD sample, the spectra clearly exhibit substrate-related features at wavelengths below 400 nm (see ESI; Fig. S1†), indicating the limited thickness of these PNIPAM films. For the MD and HD samples, the spectra for dry samples show large

‡ The lateral photodetector sensitivity was attempted to be determined by pressing the colloidal probe against a vertical rigid step of ~650 nm height microfabricated on a silicon substrate. This procedure was successfully applied to large beads of ~70 μm diameter, for instance.[55,56] However, in our case, various factors hindered the application of this procedure. These factors include the small colloidal probe size (~900 nm diameter), and uncertainties of sample tilt and of the contact point between the colloidal probe and the step edge which lead to an unknown length of the torsional moment arm.

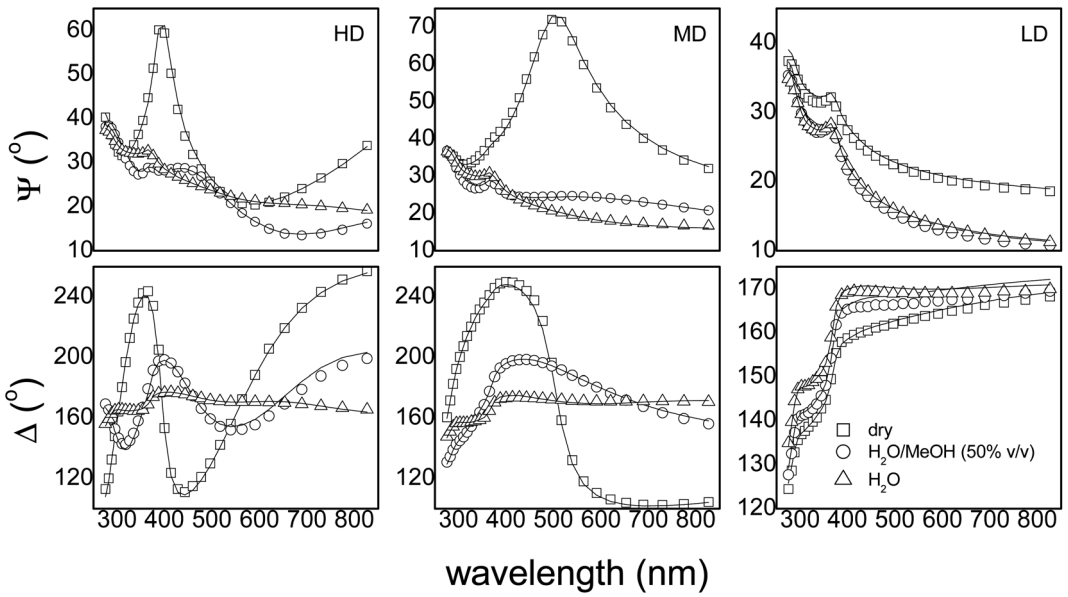

Fig. 1 Ellipsometry spectra Ψ and Δ as a function of wavelength for PNIPAM brushes with different grafting densities in various solvents. The solid lines represent fitted spectra as described in the text.

variations of both Ψ and Δ. These originate from interference of light reflected at both sides of the PNIPAM film, *i.e.* at the substrate–brush and brush–air interfaces. For the HD sample, even multiple oscillations in the spectra are observed, indicating a larger thickness of this film as compared to the MD film.

For all PNIPAM grafts, the spectra changed considerably when brought into contact with a liquid. One obvious cause is the higher refractive index of the liquid as compared to that of air. The spectral changes upon immersion show a significant contribution from polymer chain rearrangement within the PNIPAM film with respect to the dry state. For example, for the HD sample, oscillations in Ψ and Δ are still observed, although their amplitude is markedly reduced as compared to that of the dry film. For the films in water, the interference is vaguely discernible.

For all grafting densities, the spectra of films in water exhibit marked similarities to those of the bare silicon substrate (see ESI; Fig. S1†). Owing to the large swelling of the grafts in water, in combination with their reduced density, the contribution of the PNIPAM to the optical spectra becomes hard to distinguish from that of the solvent. In other words, the refractive index of the swollen samples is a combination of the refractive index of the solvent, *i.e.* water, and the dissolved PNIPAM macromolecules. Owing to the low segment density in the highly swollen brush, its effective refractive index is close to the value of the pure solvent. We finally note, that a detailed analysis of the temperature-dependent ellipsometric response of PNIPAM grafts in contact with a good solvent (water) was described in considerable detail in our previous article.[50]

To adequately model the optical properties of the grafts in the water–methanol (50% v/v) mixed solvent, we start with the graded profile of the optical parameters, *i.e.* the refractive index corresponding to a PNIPAM density gradient, for water-swollen films; the density profiles for HD and MD films in water are represented by the dashed lines in Fig. 2.

Upon replacing the liquid with the co-nonsolvent mixture we assume that the dense layer at the substrate–brush interface remains collapsed and essentially unchanged; we only consider changes in the profile of the diluted layer. Although it turns out to be not entirely unambiguous to discriminate between various models, a good fit to the ellipsometry spectra (solid lines in Fig. 1) was obtained by taking into consideration a symmetric segment density profile for the outer layer.

For larger distances in the surface-normal direction (from the substrate side), the segment density in the film interior first exhibits a decay, but rises markedly toward the outer part of the layer. The profiles for HD and MD brushes are shown in Fig. 2 by the solid lines; specific details pertaining to the model including fit parameters are provided in the ESI.†

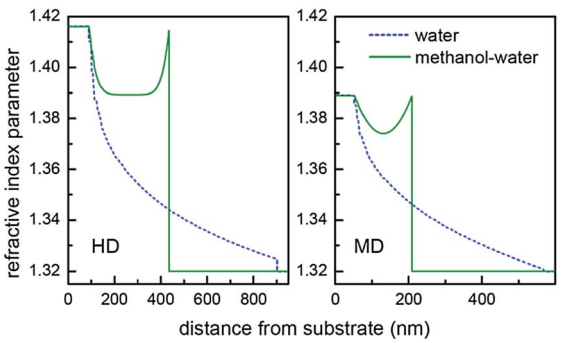

Fig. 2 Density profiles as a function of distance from the substrate for HD (left) and MD (right) PNIPAM brush samples, as determined from the refractive index gradient model as described in the text. Results are shown for brushes immersed in pure water (blue, dashed lines) and in co-nonsolvent mixtures of methanol and water (green, solid lines) at room temperature.

In addition, we would like to stress here that the collapse in mixed solvents is definitely different as compared to the temperature-induced collapse. In our previous publication[50] in which we describe the optical transition during the thermally induced collapse, ellipsometry spectra throughout the transition were analysed. The collapse induced by the mixed solvent as we studied in the present work gives rise to ellipsometry spectra which are markedly different than any of those measured during the temperature scan (see the ESI; Fig. S7†).

Thickness values for dry films, hydrated brushes in water and partially collapsed layers in co-nonsolvent mixtures, as derived from the analysis of the spectra, are summarized in Fig. 3. As mentioned, details of the analysis as well as specific fit parameters are given in the ESI.† For dry films, the ability to model the optical response using a single homogeneous Cauchy model indicates that the films consist of densely packed, collapsed layers. Upon immersion into liquids, the thickness values clearly reveal that the PNIPAM grafts in water exhibit considerable swelling. We note that the thickness values were obtained in sequence by measuring first dry films, then films swollen in water, and finally, when these swollen films were brought in contact with a 50–50% v/v water–methanol mixture. As data show, the values of the swelling ratios are strongly dependent on the grafting density. Actual values are summarized in Table 1; the swelling ratio is defined as the relative thickness increase with respect to the dry thickness. Grafts immersed in a mixture of water–methanol (50% v/v) still exhibit swelling in comparison with the corresponding dry films, but less pronounced as compared to films swollen in pure water.

Based on the above assumptions we reason that the water-swollen brushes, when brought into contact with a large excess of co-nonsolvent exhibit quick collapse in the brush contact zone with the co-nonsolvent. This collapsed layer forms a densely packed zone in the brush, which acts as barrier for the further diffusion of methanol into the water-swollen film. Eventually, a static situation is established within the partly swollen PNIPAM graft. We stress that this most likely does not correspond to an equilibrium but constitutes a kinetically stabilized conformation of the layer; however, within the time-frame of our experiments, typically 10–30 minutes, we have not been able to detect any evolution with time.

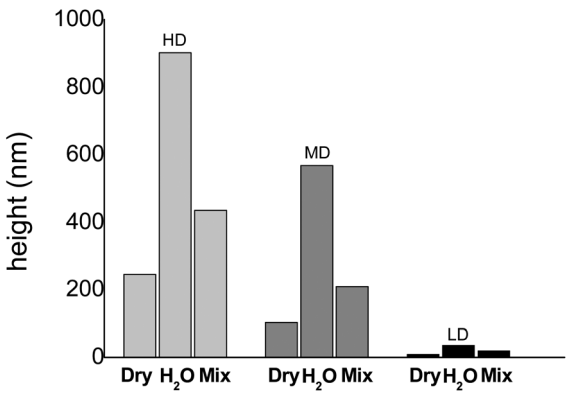

Fig. 3 Thickness of PNIPAM layers with different grafting densities plotted as a function of solvent conditions (determined from ellipsometry measurements).

Table 1 Swelling ratios (*i.e.* $(d_{imm} - d_{dry})/d_{dry}$ where d_{dry} and d_{imm} are the thicknesses of the dry and immersed films) for the different PNIPAM brushes in water and in the mixed solvent

Solvent	HD	MD	LD
Water	2.67	4.50	3.07
Water–methanol	0.77	1.03	1.26

It is interesting to consider the question of solvent composition within the films, and the solvent–segment clustering within the films. Solvents, or solvent mixtures in polymer–solvent systems often exhibit non-random partitioning and cluster formation.[61] The Kirkwood–Buff (KB) theory provides a framework to describe the solvent structure and molecular clustering by so-called KB cluster integrals (KBI)[62] in terms of molecular pair correlation functions. In water–methanol mixtures KBI-s were calculated as a function of composition and excess (or deficit) number of molecules around a central molecule were determined.[63] By the presence of bonding sites on PNIPAM chains preferring bonding of water (or methanol) the equilibrium in the solvent mixture is perturbed by polymer segment–solvent partition. Although an issue of still some debate, a widely accepted view assumes that preferential adsorption of methanol to polymer chains in the mixed water–methanol system is the main contributor to the re-entrant coil-globule-coil transition in the mixed solvent of water–methanol. Solvation of PNIPAM is then related to the formation of competitive hydrogen bonds between polymer segment–water and polymer segment–methanol. Macromolecular crowding in the brush thus breaks up the solvent cluster structure, and free unclustered water molecules become available, which can swell the brush. We speculate that this residual water causes the partial de-swelling of the films in contact with the co-nonsolvent, observed by ellipsometry. We note that when the films are dried following contact with co-nonsolvents, the swelling behaviour (high swelling first in contact with water, and partial collapse when in contact with water–methanol) is fully reproducible.

Film surface nanotribology across the re-entry transition: AFM friction measurements

Following the discussion of the ellipsometry results, we shall now focus on friction characterization of the PNIPAM brushes, comparing swollen and top-collapsed films. We note, that in our previous work[39] we discussed the variation of friction force for swollen and temperature collapsed brushes, and showed that the temperature collapse proceeds from the contact area with the substrate (high segment density), whereby the segment gradient is decreasing towards the free side of the grafts.

Friction–load plots of the polymer grafts in different liquids were recorded by friction force microscopy (FFM). FFM is a variant of AFM in which lateral deflections of the cantilever are measured as the probe attached to the cantilever slides across

the sample surface.[64] Here, microsphere probes were employed to avoid the extreme contact pressures encountered with typical sharp probes.[65] Friction images of the MD PNIPAM sample were recorded using a SiO_2 microsphere under different solvent environments by disabling the slow scan axis, thereby continuously scanning a line profile. As the brush layers are very uniform in height and lateral homogeneity revealing low roughness,[39] we assume that effects due to lateral drift of the AFM can be neglected and that the obtained line scans are representative for the friction properties of the brush layer.

The friction increases with increasing applied load in both cases, albeit to a different extent revealing a ~20 fold larger friction for the collapsed brush layer (Fig. S8, in the ESI†). Based on the friction data, friction-load plots were constructed and are shown in Fig. 4. The lateral photo-detector signal, transferred into a value for the frictional force as outlined in the calibration section in the ESI,† was plotted as a function of the applied load. The friction force exhibited a linear relationship with the load, indicative of Amontonian behavior:[66]

$$F_F = \mu N$$

where F_F is the friction force, N is the normal contact force which includes the applied load and the adhesion force between the sample and the probe, and μ is the coefficient of friction. In this paper all the friction force *vs.* load graphs have already taken the adhesion between the colloidal probe and the film surface into account and the whole curves were offset to the origin position. We found that the friction coefficient of the MD PNIPAM sample in water ($\mu = 0.23 \pm 0.01$) is five times lower than the value of the friction coefficient in the water–methanol (50% v/v) mixture ($\mu = 1.07 \pm 0.06$),[67,68] indicating a much better lubrication of the grafts in water. The excellent lubrication properties of surface tethered polymer grafts in good solvents has been reported and demonstrated to facilitate sliding between two contacting planar surfaces.[69,70] In our case, swollen PNIPAM grafts in the pure solvents water and methanol also show lubricating properties, as reflected by the low friction coefficients. In contrast, we observed high friction coefficients of $\mu = 1.55 \pm 0.05$ and $\mu = 1.07 \pm 0.06$ for high (HD) and medium (MD) brush densities (Fig. 5), exclusively in the water–methanol (50% v/v) solvent mixture. For collapsed high density PNIPAM brushes Tsujii *et al.* found a friction coefficient μ of ~2 at $T = 40$ °C by colloidal probe AFM.[71] Zauscher *et al.* investigated PNIPMAM gels by rheometry.[34] They found that gels in a collapsed conformation above the LCST revealed significantly more friction than swollen gels below the LCST at low shear rates. In a previous study,[39] we found that the interaction between the SiO_2 colloidal probe and the PNIPAM surface was repulsive when the polymer was swollen, while it became attractive and jump-to-contact behavior was observed when the solvent environment was changed to a water–methanol (50% v/v) mixture. Strong adhesion forces were recorded for all brushes in the co-nonsolvent, ranging from ~11 nN (LD) to ~16.5 nN (MD) to ~18 nN (HD). These findings support the high friction coefficients in the co-nonsolvent, in particular for the HD brush. In general, the effect of solvent on the tribological properties of polymer grafts has been studied by various groups.[53,65,72,73] It has been suggested that a high coefficient of friction is associated with the collapsed conformation of polymer grafts, while extended conformations confer a significantly reduced friction force due to the changes in adhesion and energy dissipation.[53,65,72,73] In the solvent mixture brushes collapse and stiffen accordingly. Consequently they lose their lubrication properties and this causes viscoelastic losses during friction and the high friction coefficients. On rubbery materials lubricated and non-lubricated friction was studied in great detail. Non-lubricated friction caused high viscoelastic losses leading to high friction coefficients $\gg 1$.[74,75] The data shown in Fig. 4 are in good qualitative agreement with these studies. In conclusion, for the collapsed grafts the layer contains disordered chains in which the molecular conformational changes may readily be induced during "ploughing". In contrast, the swollen grafts retain substantial lubricity because the bound solvent molecules prevent significant deformation of the extended chains and reduce the extent of energy dissipation at a given load.

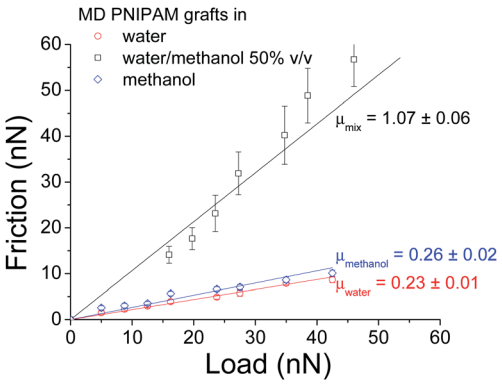

Fig. 4 Friction of the MD PNIPAM sample as a function of load in different solvents as indicated in the legend.

Friction measurements were then carried out on LD and HD PNIPAM grafts as well. For the HD PNIPAM sample, the coefficient of friction increased by a factor of 4 on switching from water to water–methanol (50% v/v). In contrast, for LD PNIPAM the friction coefficient remained almost the same. As can be seen in Fig. 3, the thickness of the LD brush is substantially lower (one order of magnitude) as compared to those of the HD and MD brushes. We previously found significant adhesion between the colloidal probe and the LD brush surface in the co-nonsolvent.[39] We believe that the ultrathin PNIPAM film also exposed parts of the silicon substrate, resulting in contact area heterogeneity.

As mentioned earlier, the frictional properties of PNIPAM grafts depend strongly on the extent of swelling. To demonstrate the reversibility of the conformation change corresponding to the swelling and determine the transition kinetics, the solvent environment of the HD PNIPAM sample was changed *in situ* while the friction image was recorded in real-time. The obtained friction image and cross-section analysis are shown in Fig. 6a. The photodetector response of the HD PNIPAM sample shifted between the two states as the solvent

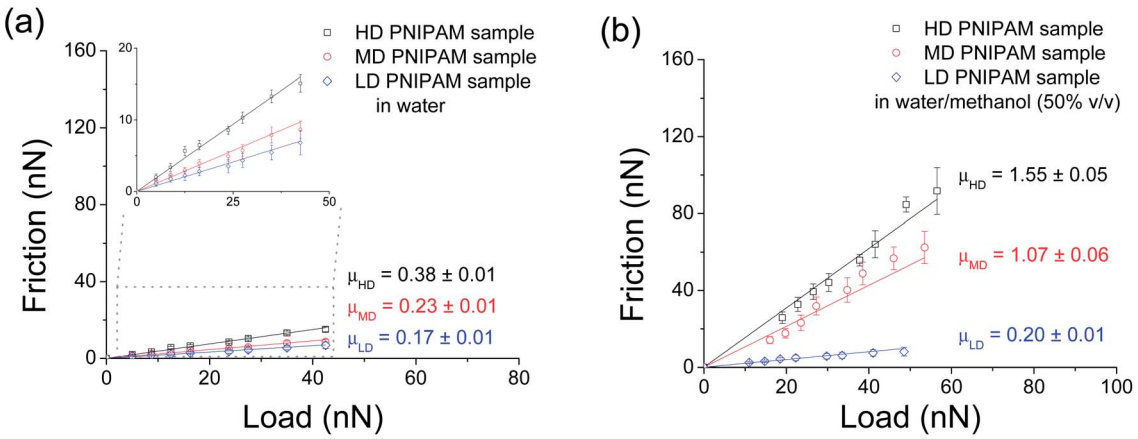

Fig. 5 Friction of PNIPAM layers with different grafting densities as a function of load in (a) water and (b) water–methanol (50% v/v). Solid lines are least square fits to the data.

environment was cycled between water and water–methanol (50% v/v), indicating the reversibility of the process. The slight offset between the first and the second cycle could be induced by the piezo-movement as resulted from the brush height difference. From the cross-section analysis (Fig. 6b) we can see that the friction increased gradually when the co-nonsolvent was introduced (grey bar). The increase was fit to an exponential function and a typical decay time $\tau = 26.7 \pm 2.4$ s was found. The same experiments were carried out on MD (Fig. 6c) and LD (Fig. 6d) samples. The MD brush showed behaviour similar to that of the HD brush, the decay time for the MD sample was determined to be 23.1 ± 2.9 s. No change in friction

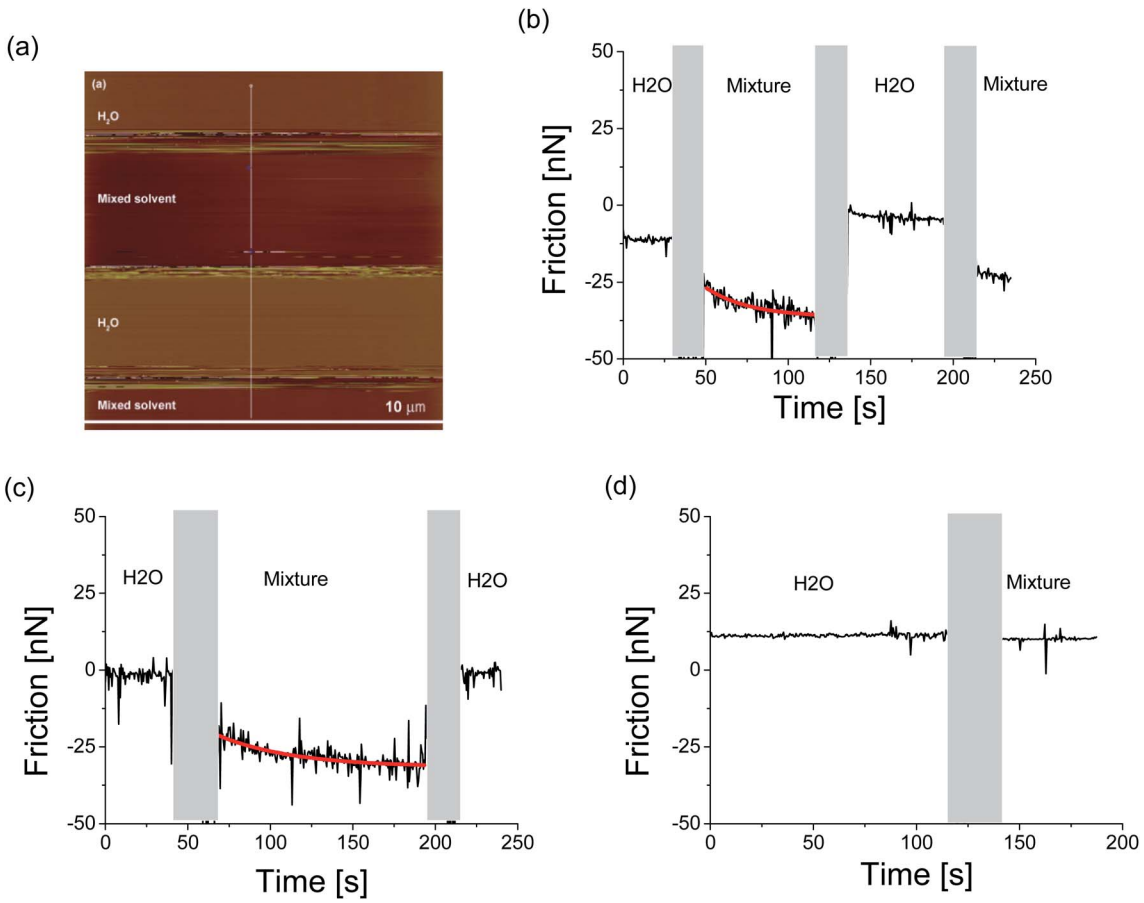

Fig. 6 (a) AFM friction image of the HD PNIPAM sample. The solvent was changed from water to water–methanol 50% v/v as indicated in the image. (b) Cross-section of the white vertical line in (a). Cross-sections of the (c) MD and (d) LD PNIPAM samples are also shown. The grey bars indicate the equilibrium time between the solvent exchanges. The solid lines in (b) and (c) are exponential decay fits to the data.

was found in the case of the LD sample. The transition dynamics of PNIPAM grafts from the swollen to the collapsed state was previously followed by monitoring the adherence change with AFM. The results obtained in this study were well in line with the timescale observed by following the variation of adherence in the previous paper.[37] This indicates that the change in friction due to variation in solvent composition has likely the same mechanism as in the change of adherence. This change is attributed to the diffusion of solvent molecules into (or out of) the PNIPAM brushes in the previous paper. In the case of a thicker polymer layer, more time is needed for solvent exchange to take place as the collapsed outer layer serves as a diffusion barrier. Here by the complementary study of friction, solvent diffusion is further proven to be related to the change in the properties of the PNIPAM layers. We believe that the transition kinetics of polymer grafts responses to solvent change as demonstrated here provides important information for the use of these kinds of materials and applications.

Conclusions

PNIPAM layers with three different grafting densities were synthesized *via* surface-initiated atom transfer radical polymerization (SI-ATRP). The response of these grafts to immersion in a good solvent and in co-nonsolvent mixtures was studied. Variations in the layer thickness and segment density distribution due to changes in the solvent environment were monitored by *in situ* ellipsometry. Quantitative analysis yields an adequate model to describe the ellipsometry spectra. The swelling ratio was found to be strongly dependent on the grafting density. Grafts immersed in the co-nonsolvent, *i.e.* a mixture of methanol and water, still exhibited swelling, but less pronounced as compared to pure water. In fact, the ellipsometry model suggests a limited collapse of the film interior, which partially remains hydrated, combined with a more densely collapsed outer layer on the solvent side.

Analysis of the AFM based lateral force measurements, using the structural model as derived from the ellipsometry measurements, revealed low friction forces in water, which greatly increased in water–methanol (50% v/v) for the medium and high density brushes; friction coefficients values exceeding 1 were found. The observed friction response was fully reversible, while the quantitative friction characterization is in agreement with the structural model proposed on the basis of the optical response. The collapse dynamics of the PNIPAM grafts was also investigated by monitoring the change of friction between the graft surface and the colloidal probe with the introduction of the co-nonsolvent.

Acknowledgements

We thank the MESA$^+$ Institute for Nanotechnology, and the Netherlands Organization for Scientific Research (NWO, TOP Grant 700.56.322, Macromolecular Nanotechnology with Stimulus Responsive Polymers) for financial support.

Notes and references

1 R. Barbey, L. Lavanant, D. Paripovic, N. Schuwer, C. Sugnaux, S. Tugulu and H. A. Klok, *Chem. Rev.*, 2009, **109**, 5437–5527.
2 P. M. Mendes, *Chem. Soc. Rev.*, 2008, **37**, 2512–2529.
3 S. Edmondson, V. L. Osborne and W. T. S. Huck, *Chem. Soc. Rev.*, 2004, **33**, 14–22.
4 K. Matyjaszewski and N. V. Tsarevsky, *Nat. Chem.*, 2009, **1**, 276–288.
5 S. Minko, *Polym. Rev.*, 2006, **46**, 397–420.
6 M. A. C. Stuart, W. T. S. Huck, J. Genzer, M. Muller, C. Ober, M. Stamm, G. B. Sukhorukov, I. Szleifer, V. V. Tsukruk, M. Urban, F. Winnik, S. Zauscher, I. Luzinov and S. Minko, *Nat. Mater.*, 2010, **9**, 101–113.
7 Y. Tsujii, K. Ohno, S. Yamamoto, A. Goto and T. Fukuda, *Adv. Polym. Sci.*, 2006, **197**, 1–45.
8 G. J. Vancso, X. F. Sui, S. Zapotoczny, E. M. Benetti and P. Schon, *J. Mater. Chem.*, 2010, **20**, 4981–4993.
9 O. Smidsrod and J. E. Guillet, *Macromolecules*, 1969, **2**, 272–277.
10 H. G. Schild, *Prog. Polym. Sci.*, 1992, **17**, 163–249.
11 K. N. Plunkett, X. Zhu, J. S. Moore and D. E. Leckband, *Langmuir*, 2006, **22**, 4259–4266.
12 E. Kutnyanszky, A. Embrechts, M. A. Hempenius and G. J. Vancso, *Chem. Phys. Lett.*, 2012, **535**, 126–130.
13 I. Luzinov, S. Minko and V. V. Tsukruk, *Soft Matter*, 2008, **4**, 714–725.
14 G. J. Vancso, X. F. Sui, S. Zapotoczny, E. M. Benetti, M. Memesa and M. A. Hempenius, *Polym. Chem.*, 2011, **2**, 879–884.
15 E. S. Alla Synytska, N. Puretskiy, G. Stoychev, S. Berger, L. Ionov, C. Bellmann, K.-J. Eichhorn and M. Stamm, *Soft Matter*, 2010, **6**, 5907.
16 N. Ishida and S. Biggs, *Macromolecules*, 2010, **43**, 7269–7276.
17 E. M. Benetti, S. Zapotoczny and J. Vancso, *Adv. Mater.*, 2007, **19**, 268–271.
18 E. C. Cho, Y. D. Kim and K. Cho, *J. Colloid Interface Sci.*, 2005, **286**, 479–486.
19 M. A. Cole, N. H. Voelcker, H. Thissen, R. G. Horn and H. J. Griesser, *Soft Matter*, 2010, **6**, 2657–2667.
20 N. Ishida and S. Biggs, *Langmuir*, 2007, **23**, 11083–11088.
21 D. M. Jones, J. R. Smith, W. T. S. Huck and C. Alexander, *Adv. Mater.*, 2002, **14**, 1130–1134.
22 S. Kidoaki, S. Ohya, Y. Nakayama and T. Matsuda, *Langmuir*, 2001, **17**, 2402–2407.
23 G. Liu and G. Zhang, *J. Phys. Chem. B*, 2005, **109**, 743–747.
24 I. B. Malham and L. Bureau, *Langmuir*, 2010, **26**, 4762–4768.
25 S. Mendez, B. P. Andrzejewski, H. E. Canavan, D. J. Keller, J. D. McCoy, G. P. Lopez and J. G. Curro, *Langmuir*, 2009, **25**, 10624–10632.
26 H. Yim, M. S. Kent, S. Mendez, G. P. Lopez, S. Satija and Y. Seo, *Macromolecules*, 2006, **39**, 3420–3426.
27 X. Zhu, C. Yan, F. M. Winnik and D. Leckband, *Langmuir*, 2007, **23**, 162–169.
28 F. M. Winnik, H. Ringsdorf and J. Venzmer, *Macromolecules*, 1990, **23**, 2415–2416.

29 H. M. Crowther and B. Vincent, *Colloid Polym. Sci.*, 1998, **276**, 46–51.
30 H. G. Schild, M. Muthukumar and D. A. Tirrell, *Macromolecules*, 1991, **24**, 948–952.
31 I. Anac, A. Aulasevich, M. J. N. Junk, P. Jakubowicz, R. F. Roskamp, B. Menges, U. Jonas and W. Knoll, *Macromol. Chem. Phys.*, 2010, **211**, 1018–1025.
32 M. Kaholek, W. K. Lee, S. J. Ahn, H. W. Ma, K. C. Caster, B. LaMattina and S. Zauscher, *Chem. Mater.*, 2004, **16**, 3688–3696.
33 G. M. Liu and G. Z. Zhang, *Langmuir*, 2005, **21**, 2086–2090.
34 D. P. Chang, J. E. Dolbow and S. Zauscher, *Langmuir*, 2007, **23**, 250–257.
35 F. Tanaka, T. Koga, H. Kojima, N. Xue and F. M. Winnik, *Macromolecules*, 2011, **44**, 2978–2989.
36 F. Tanaka, T. Koga and F. M. Winnik, *Phys. Rev. Lett.*, 2008, **101**, 028302.
37 F. Tanaka, T. Koga, H. Kojima and F. A. Winnik, *Macromolecules*, 2009, **42**, 1321–1330.
38 P. W. Zhu and D. H. Napper, *J. Colloid Interface Sci.*, 1996, **177**, 343–352.
39 X. F. Sui, Q. Chen, M. A. Hempenius and G. J. Vancso, *Small*, 2011, **7**, 1440–1447.
40 Spectroscopic ellipsometry involves the measurement of the optical response in terms of ellipsometric parameters over a wide spectral range.
41 A. Takahara, M. Kobayashi, Y. Terayama, N. Hosaka, M. Kaido, A. Suzuki, N. Yamada, N. Torikai and K. Ishihara, *Soft Matter*, 2007, **3**, 740–746.
42 M. K. Vyas, K. Schneider, B. Nandan and M. Stamm, *Soft Matter*, 2008, **4**, 1024–1032.
43 A. J. Morse, S. Edmondson, D. Dupin, S. P. Armes, Z. Zhang, G. J. Leggett, R. L. Thompson and A. L. Lewis, *Soft Matter*, 2010, **6**, 1571–1579.
44 S. Edmondson, N. T. Nguyen, A. L. Lewis and S. P. Armes, *Langmuir*, 2010, **26**, 7216–7226.
45 H. Tu, C. E. Heitzman and P. V. Braun, *Langmuir*, 2004, **20**, 8313–8320.
46 S. B. Rahane, J. A. Floyd, A. T. Metters and S. M. Kilbey, *Adv. Funct. Mater.*, 2008, **18**, 1232–1240.
47 S. Q. Wang and Y. X. Zhu, *Langmuir*, 2009, **25**, 13448–13455.
48 C. Y. Xue, N. Yonet-Tanyeri, N. Brouette, M. Sferrazza, P. V. Braun and D. E. Leckband, *Langmuir*, 2011, **27**, 8810–8818.
49 L. Patra, A. Vidyasagar and R. Toomey, *Soft Matter*, 2011, **7**, 6061–6067.
50 E. S. Kooij, X. F. Sui, M. A. Hempenius, H. J. W. Zandvliet and G. J. Vancso, *J. Phys. Chem. B*, 2012, **116**, 9261–9268.
51 H. J. Butt, B. Cappella and M. Kappl, *Surf. Sci. Rep.*, 2005, **59**, 1–152.
52 H. Schonherr, E. Tocha and G. J. Vancso, *Top. Curr. Chem.*, 2008, **285**, 103–156.
53 N. Nordgren and M. W. Rutland, *Nano Lett.*, 2009, **9**, 2984–2990.
54 Z. Y. Zhang, A. J. Morse, S. P. Armes, A. L. Lewis, M. Geoghegan and G. J. Leggett, *Langmuir*, 2011, **27**, 2514–2521.
55 E. D. Palik, O. J. Glembocki, I. Heard, P. S. Burno and L. Tenerz, *J. Appl. Phys.*, 1991, **70**, 3291–3300.
56 J. L. Hutter and J. Bechhoefer, *Rev. Sci. Instrum.*, 1993, **64**, 1868–1873.
57 Y. Kondoh, J. Seeger and P. Merchant, *J. Microelectromech. Syst.*, 1998, **7**, 428–434.
58 J. E. Sader, *Rev. Sci. Instrum.*, 2003, **74**, 2438–2443.
59 E. Tocha, H. Schonherr and G. J. Vancso, *Langmuir*, 2006, **22**, 2340–2350.
60 R. M. A. Azzam and N. M. Bashara, *Ellipsometry and Polarized Light*, Elsevier Science Ltd, 1987.
61 Z. J. Tan and G. J. Vancso, *Macromolecules*, 1997, **30**, 4665–4673.
62 J. G. Kirkwood and F. P. Buff, *J. Chem. Phys.*, 1951, **19**, 774–777.
63 I. L. Shulgin and E. Ruckenstein, *J. Phys. Chem. B*, 2006, **110**, 12707–12713.
64 R. W. Carpick and M. Salmeron, *Chem. Rev.*, 1997, **97**, 1163–1194.
65 M. A. Brady, F. T. Limpoco and S. S. Perry, *Langmuir*, 2009, **25**, 7443–7449.
66 X. T. Liu, E. Thormann, A. Dedinaite, M. Rutland, C. Visnevskij, R. Makuskac and P. M. Claesson, *Soft Matter*, 2013, **9**, 5361–5371.
67 D. V. Vezenov, A. Noy, L. F. Rozsnyai and C. M. Lieber, *J. Am. Chem. Soc.*, 1997, **119**, 2006–2015.
68 A. Noy, D. V. Vezenov and C. M. Lieber, *Annu. Rev. Mater. Sci.*, 1997, **27**, 381–421.
69 J. Klein, E. Kumacheva, D. Mahalu, D. Perahia and L. J. Fetters, *Nature*, 1994, **370**, 634–636.
70 R. Tadmor, J. Janik, J. Klein and L. J. Fetters, *Phys. Rev. Lett.*, 2003, **91**, 115503.
71 Y. Tsujii, A. Omura, K. Okayasu, W. Gao, K. Ohno and T. Fukuda, *J. Phys.: Conf. Ser.*, 2009, **184**, 012031.
72 F. T. Limpoco, R. C. Advincula and S. S. Perry, *Langmuir*, 2007, **23**, 12196–12201.
73 A. Li, S. N. Ramakrishna, E. S. Kooij, R. M. Espinosa-Marzal and N. D. Spencer, *Soft Matter*, 2012, **8**, 9092–9100.
74 J. A. Greenwood and D. Tabor, *Proc. Phys. Soc., London*, 1958, **71**, 989–1001.
75 D. Kaneko, M. Oshikawa, T. Yamaguchi, J. P. Gong and M. Doi, *J. Phys. Soc. Jpn.*, 2007, **76**, 014602.

